Recyclable Nonfunctionalized Paper-Based Ultralow-Cost Wearable Health Monitoring System

WILEY-VCH

DOI: 10.1002/ ((please add manuscript number))
Article type: Full Paper

Title: Recyclable Non-functionalized Paper Based Ultra-Low Cost Wearable Health Monitoring System

*Joanna M. Nassar[1], Kush Mishra[1], Kirklann Lau[1, 2], Andres A. Aguirre-Pablo[3] and Muhammad M. Hussain[1]**

J. M. Nassar, Kush Mishra, Kirk Lau, Prof. M. M. Hussain
[1]Integrated Disruptive Electronic Applications (IDEA) Lab and Integrated Nanotechnology Lab, Computer Electrical Mathematical Science and Engineering Division, King Abdullah University of Science and Technology (KAUST), Thuwal 23955-6900, Saudi Arabia

Kirk Lau
[2]Harvey Mudd College, Claremont, CA 91711, USA

Andres A. Aguirre-Pablo
[3]High Speed Fluids Imaging Lab, Physical Sciences and Engineering, Mechanical Engineering, Physical Science and Engineering Division, King Abdullah University of Science and Technology (KAUST), Thuwal 23955-6900, Saudi Arabia

Corresponding author's e-mail: muhammadmustafa.hussain@kaust.edu.sa

Keywords: Paper, Monitoring system, Healthcare, Sensors.

Abstract - In recent years, innovation in wearable health monitors has surged from significant advances in flexible sensory arrays, wireless technologies, and scaled low-power electronics. Such biometric monitoring devices are critical for continuous monitoring of body vitals and health conditions as means of care for advanced personalized healthcare. Still, widespread deployment of such devices are far more remote due to affordability (viz. complex materials and processes induced higher price), low sensitivity, selectivity, recovery and disposability. Therefore, in addition to functionality, accuracy, comfort and convenience, affordability and accessibility are critical need for the wide adaptation of its benefits. Here we show an integration strategy to rationally design an ultra-low cost health monitoring device, a "Paper Watch", using recyclable household materials: non-functionalized papers. Its unusual simplicity in manufacturing and in daily use, gives it unprecedented

edge compared to any previous demonstrations. We integrate pressure, temperature and humidity sensors with flexible silicon ICs on one singular platform, with demonstrated reliability under physical deformation, which for the first time can sense the body vitals of the carrier (body temperature, blood pressure, heart rate, and skin hydration) simultaneously and in real-time. Our goal is to show that limitless possibilities exist to innovate and to advance low-cost healthcare technology for multitude of applications.

1. Introduction

Wearable health monitors are getting increased popularity as a bridge to future personalized advanced healthcare. Constant monitoring of body vitals and other important metrics enable digitized accurate monitoring of one's health, early detection of any potential fatal illness, incessant monitoring of sensitive illnesses and definitely enhancing wellness. Thus today's wearable gadgets are being developed to monitor vital signs continuously and as non-invasively and comfortably as possible [1-13]. As an example, such devices can potentially save a person from enduring a sudden heart attack. In fact, premature signs of heart disease can be identified from two or more of the following signs happening together: ventricular contractions, high blood pressure, unusual high arterial stiffness, unusual sweating, the manifestation of 6 heartbeats per minute (bpm), or a resting pulse reading more than 100 bpm[1]. These signs can occur within seconds, minutes and even days before the actual event of a heart attack, early enough to take action and go to the hospital.

However, today's wearable health monitors are expensive and thus their deployment is limited to a small group of financially privileged population. Additionally, they are bulky and rigid, limited by conventional state-of-the-art silicon-based Integrated Circuits (ICs), making them uncomfortable for continuous wear and detection. We witness a range of commercial devices in the form of smart watch, wrist band, or smartphones, mainly targeted at monitoring fitness signs and track activity (*viz.* heart rate sensor and pedometer). Nevertheless, no such devices can offer the ability to perform proper medical diagnostics, mainly constrained by the non-intimate interface between the physical sensors

and the skin. Thus, efforts are being implemented to improve these devices by incorporating flexible sensors to develop wearable health monitors with three main aspects to consider: (i) complete flexibility to provide comfort and adaptability to the body, (ii) intimate interface with the skin for proper body sensing, and (iii) non-invasive attachment technique. Following these characteristics, new fabrication techniques and materials using intrinsically flexible and lightweight materials (e.g. plastic and elastomers) are being used in emerging flexible sensors viable for implementation in continuous vital signs detection[2, 14-19]. The flexibility of the wearable device allows conformal placement on curvilinear areas of the body, such as wrapping around the arm, the wrist, or placement on the chest for respiration rate tracking. Unfortunately, scholarly advances in wearable health monitors use very expensive and complex sensing materials, such as graphene-based strain sensors[20], nanowire-based (NWs) pressure sensors[21], and carbon nanotubes (CNTs) sensory systems[22], leading to a significant increase in the cost of the sensory arrays. Therefore, accessibility to advanced but simple and low-cost healthcare monitoring systems becomes one of the key engineering challenges of the 21st century.

Meanwhile, when it comes to full system integration, silicon-based electronics are absolute necessities for data management. Printed transistors cannot perform such high performance complex tasks required by even a modest sensory system. Nevertheless, printing is suitable for sensors as they solely require conductive and insulating materials. Therefore, the ideal design for a wearable health monitoring device would take a hybrid approach where advanced flexible materials (e.g. polymers or paper) are integrated in conjunction with flexible silicon integrated circuits (ICs). A similar methodology was shown by Javey *et al.*[23] for an autonomous "smart wristband", integrating biochemical sensors with rigid off-the-shelf processing units on a flexible printed circuit board. However, such sophisticated chemical functionalized based complex "semi-flexible" approach reveals complexity in use for interchangeable sensor electrodes, unwanted stress, localized strain, and hot spots in contact with the human skin[24], leading to weak spots around the bonded ICs and an overall reduction in the system's reliability and safety[24]. As an alternative, here we show an

integrated approach where thinned down flexible bulk monocrystalline Si (100) based data processing units are integrated on paper substrates **(Figure 1)**. The flexible silicon ICs display improved system flexibility, reduced accumulated stress, and lower heating effect on the skin[24]. Our vision towards an autonomous wearable device is to replace the flexible printed circuit board with printed stretchable metal-interconnects on a low-cost paper platform **(Figure 1),** where careful integration and alignment of flexible processing units is performed through flip-chip technique. Compared to previous demonstrations[23], our system uses recyclable papers instead of chemically treated materials, displays a simpler and affordable integration approach, improved contact intimacy with the skin, and exhibits a smaller footprint on the environment. Also paper has been in use in our daily life for centuries and thus its manufacturability, simplicity and authenticity is beyond doubt. Accordingly, the autonomous health monitoring system displays a 3D stacked structure **(Figure 1)**, where the layers are vertically interconnected through conductive vias as demonstrated by a similar approach shown by Whitesides *et al.*[25] The top layer represents an active RFID tag for radio communication, printed using silver ink pen on Post-it paper and integrating a flexible radio chip. The layer below embodies the power management circuitry and the third layer contains the main processing unit using thinned down silicon-based microprocessor (μP)[26]. The next layer contains the sensors' readout circuitry, and the last layer illustrates an in-plane integration of multifunctional sensors for monitoring bio signals such as body temperature, sweating, heart rate, respiration, and blood pressure **(Figure 1).** Note that the sensors are employed face down for direct contact with the human skin. This intimate placement is necessary for collecting body vitals, where otherwise the sensors would collect information from the surrounding environment. Finally, the system is interfaced with a smartphone, where data is wirelessly collected, interpreted, and visualized. This procedure is cost-effective, flexible, lightweight and safely conformal to the body of the carrier.

With this approach, we show the use of paper-based sensors in various healthcare applications, such as basic real-time symptoms and illness detection. The developed multisensory platform uses affordable and recyclable household materials such as paper and aluminum foil. In a previous report,

we demonstrated the development of the first ever affordable Paper Skin for simultaneous environmental stimuli detection, consisting of a 3D stacked configuration[27]. In this work, we use the same set of material systems to integrate pressure, temperature and humidity sensors using an in-plane monolithic integration, best suited to optimize detection of the carrier's vital signs. The presented "Paper Watch" is conformal to the irregularities of the human body and can be uniformly placed around the wrist with proper interface with the skin, enabling the continuous and simultaneous detection of body temperature, heart rate, blood pressure and sweating. The device delivers sufficient functionality and ease of access to monitoring and awareness system, and is specifically designed to be affordable and lightweight, fully encapsulated in a customizable flexible 3D printed wristband.

2. Materials and Methods

Using a simple fabrication process, we developed a 3.5 cm × 2.5 cm multi-sensory platform made completely out of recyclable household materials **(Figure 2a-b)**. The sensory platform integrates pressure, humidity and temperature sensors prepared solely from affordable resources such as post-it note, double-sided adhesive tape, aluminum foil, and tissue wipes, as described in **Supplementary Information** and though the fabrication flow schematic in **Figure.** An in-plane monolithic integration of the sensors is necessary for direct skin-to-sensor contact, essential for monitoring irregularities from the human body rather than the surrounding environment. The off-the-shelf materials are used as they are without any functionalization. Details about the choice of material, topography, electrical and mechanical properties can be found in **Supplementary Information** and our previous report[27], where specifics about the conductivity, porosity, compressibility, and stiffness of the materials are all discussed.

The structure, fabrication process and principle of operation of the paper sensors are thoroughly illustrated in our previous report and in **Figure 2** [27]. As overview, the pressure sensor consists of a parallel plate capacitive structure, where aluminum foil acts as the metal contact. The pressure sensing performance is affected by the viscoelasticity and porosity of the dielectric material used (*viz.* 600

µm thick microfiber wipe and 90 µm air-gap)[27] (**Figure 2c**). The polypropylene (PP) wipe illustrates a network of randomly oriented microfibril threads which improves low-pressure sensitivity, perfect for detecting tonometry pulses. Temperature and humidity sensors are simply drawn on a post-it paper using a silver ink pen. Temperature sensors consist of a simple metal resistive structure **(Figure 2a)** where resistance increases due to an increase in atomic collisions in the conductor as higher temperatures are sensed. In contrast, humidity sensors use a capacitive structure through interdigitated electrodes design **(Figure 2b).** The altered relative permittivity of the sensing film (*i.e.* Post-It™ paper) directly modifies the capacitance value, and plays a crucial role in determining the sensitivity, response and recovery times of the sensor[27].

3. Detection Mechanisms of Body Vitals

The four main vital signs to be routinely monitored are: i) body temperature, ii) sweat levels, iii) heart rate, and iv) blood pressure. Respiration rate is also important and more information about its significance and detection method is discussed in **Supplementary Information**. Typically, these bio signals are collected from different corresponding body locations. Customarily, blood pressure measurements are performed around the arm using the surface electromyography (SEMG) technique, whereas temperature, heart rate, and motion signals can be obtained from the wrist[1]. Our developed "Paper Watch" is targeted at non-invasively monitoring these different vital signs only from around the wrist.

3.1 Skin and Body Temperature

In the case of wearables and non-invasive measurement techniques, temperature measurement from the surface of the skin is quick to perform and mainly senses infrared emissions radiating from the skin. Temperature sensors are placed on the arm, chest or wrist to record temperatures less than the body-core temperature (further details found in **Supplementary Information**). For example, at room temperature (T = 25 °C), normal wrist temperature is around 32 °C while the body-core temperature

is around 37 °C[1]. Therefore, when taking temperature measurements from around the wrist, on average we need to add an extra 5 °C to have a proper body temperature value. We choose a resistance temperature detector (RTD) type of sensor, meaning when the sensor is put in direct contact with the human skin, the resistance increases in response to higher temperature detected, displaying a positive temperature coefficient of resistance (TCR). The more intimate the sensor is to our skin (i.e. direct contact of the sensor's metal layer with the skin), the less heat dissipation and the more accurate measurements we can get.

3.2 Sweating

Sweating can arise from a variety of external stimuli or health conditions, and generally, body temperature and sweating are correlated to one another (details found in **Supplementary Information**). As we start sweating as a result of the excess heat in the body, water from the surface of the skin is evaporated, making the surface of the skin more humid and covered with water droplets. In this case, sweating levels can be detected through the increase in relative permittivity of the skin's surface as it gets more humid. This can be directly sensed using our paper humidity sensor in contact with the skin, translating sweat levels into increased capacitance values (**Supplementary Information**)[27]. Therefore, in body vitals monitoring applications, it is important to have an intimate placement of the sensor, in such a way the sensing paper can react with the water droplets on the surface of the skin.

3.3 Heart Rate

Heart rate (HR) (expressed in beats per minute, bpm) changes according to the body's need and is susceptible to alterations under any major change in the physical or mental state of a person (**Supplementary Information**). Therefore, HR is used as one of the vital signs to assess a person's health condition. It can be either measured from the radial artery pulse at the wrist, from the carotid artery at the neck, or by direct contact on the chest near the heartbeats. Pressure sensors placed on the

wrist have demonstrated to be preferable over ECG for heart rate monitoring in wearable devices[1]. The sensing technique used to obtain the pulse signal from the radial artery is called Plethysmography (PPG)[5, 28]. In this work, we use paper-based pressure sensors placed either on the chest or around the wrist on the radial artery to monitor the heart rate pulses. When placed on the chest, each heartbeat will be translated into a high pressure peak due to contraction and expansion of the heart muscle. When placed around the wrist, with every heartbeat and pumping cycle, the arteries are distended. In this case, during the systolic phase (i.e. the phase of the heartbeat when the heart muscle contracts and pumps blood from into the arteries) the pressure peaks due to a high volume of blood. And the heart rate is defined as the interval between two systolic peaks. These systolic peaks are detected using pressure sensors placed either on the radial artery[5] or the carotid artery[28].

3.4 Blood Pressure

The two most significant numbers in blood pressure (BP) are the maxima (systolic) and minima (diastolic), where the BP of a healthy person lies below 120 mm Hg/80 mm Hg (systolic/diastolic), and higher blood pressures are diagnosed as hypertension. Similarly, the blood pressure is analyzed from the same radial artery pulse pressure waveform using the pressure sensor around the wrist. As each BP pulse crosses the tissue in the underlying artery, a force is exerted on the sensor. The high sensitivity, fast response and relaxation times of the sensor enable the pressure device to measure blood pressure precisely enough for arterial tonometry. One of the challenges with pulse pressure sensing is placing the sensor in the area with the strongest signal, and dealing with dampening effects. More information is found in **Supplementary Information**. Generally, the dampening of the mean blood pressure when it reaches the arteries is approximately characterized by a 50% to 70% dampening, where the mean blood pressure measured can fall down to 25 mmHg to 30 mmHg[29].

Main health issues and emotional states can be revealed through one or a combination of irregularities in the monitored vital signs. For example, sudden and unusual sweating can be translated

into a form of anxiety or related to stress-induced hyperthermia, high blood pressure and increased heart rate.

4. Interconnects Stability under Bending Conditions

In the development of wearable sensors, it is important to understand the stability and behavior of the materials under physical deformations (bending conditions), evaluating electrical variations or delamination issues which will determine the long-term stability of our sensors. In this work, we study the topographical changes in the microstructure of the silver ink when exposed to tensile strains down to a bending radius of R= 2 mm **(Figure 3)**. When the platform is concave bent, the metal layer (i.e. silver ink) undergoes slight strain, leading to a linear increase in resistance: as strain "ε" increases, resistance "r" increases following $\Delta r/r_0 = GF \times \varepsilon$, where GF is the gage factor and "r_0" is the initial resistance under no strain. **Figure S1** displays the electrical resistance "R" as a function of bending radius, highlighting a linear increase in resistance from 2.8 Ω to 4.3 Ω when bent down to 2 mm radius. Since the Post-It™ substrate is ductile, the silver layers see minimal strain [30], and no major cracks or delamination are observed. This is supported through scanning electron microscopy (SEM) images in **Figure 3** where surface topography of silver metal lines on paper are visualized under strain effects. Under no bending conditions **(Figure 3a)**, we see the typical structure expected from the metal film, displaying a hexagonal arrangement of the silver particles **(Figure 3b and c).** When the sample is bent to R = 1.5 cm **(Fig. 3d)**, again no topographical changes are observed **(Figure 3e and f)**, due to minimal strain seen by the film. As we push bend the sample further down to 2 mm **(Figure 3g)**, strain levels increase but show no major visual discontinuities at low magnification **(Figure 3h),** and at higher magnification we notice strain-induced cracks in the metal film, where the silver composites start moving away from one another along the tensile bending direction **(Figure 3i).** This behavior is expected since our metal is not a uniformly conformal 2D film, rather a superposition of Ag particles, and under high tensile strain we are likely to see minor cracks in the microstructure. To support further the stability of our sensors under bending when it is worn through time, we made a cycling test of 300 bend and unbend cycles, as seen in **Figure S2**. We took as an

example the temperature sensor and we placed it on an automatic cycling tool and ran it for 300 cycles by bending it down to a bending radius of R=1.5 cm then releasing back to original flat position. The plot in **Figure S2** clearly confirms the stability of our sensors with continuous cycling, displaying a negligible standard deviation $\sigma = 0.13$.

In general, there are no major strain-induced cracks or total discontinuities, highlighting the robustness of our stack down to 1.5 cm bending and hence we would expect robustness of the platform in the long-term as it is being worn. Since our sensory platform targets wearable healthcare monitoring applications, commonly placed on the chest (no bending – slight surface irregularity), around the arm and around the wrist, the smallest bending radius encountered would be around the wrist joint with an average bending radius down to 2 cm[31]. In fact, the average wrist circumference, including children and adults, is about 17.14 cm[31] which approximately leads to an average bending radius at the joints of 2.73 cm.

5. Real-time Monitoring of Body Vitals

The behavior and performance of the sensors have been initially studied and analyzed in our previous report[27] and are summarized in **Supplementary Information**. The paper health monitor was then employed on the chest **(Figure 4a)** and the wrist **(Figure 4b)** of a volunteer to simultaneously monitor his heart rate, blood pressure, body temperature and sweat levels in real-time.

Real-time monitoring of HR before (i.e. at rest) and after exercise (*viz.* 10 minutes run) were detected by placing the paper health monitor on the chest as close as possible to the heartbeats **(Figure 4a).** As expected, the corresponding real-time plots in **Figure 4c and d** display peaks of higher capacitance as a result of higher pressures corresponding to a heartbeat. HR is then determined as the number of heartbeats or peak pulses detected per minute. At rest, **Figure 4c** shows a resting heart rate of 62 bpm, and 95 bpm after 10 minutes of physical exercise **(Figure 4d).** Simultaneously, HR measurements were collected using the built-in heart monitor of Samsung S5 smartphone, revealing a resting HR of 60 bpm **(Figure 4c)**, and 95 bpm after exercise **(Figure 4d).** Comparing both

techniques, our measured resting pulse is within 3% of the value collected from the smartphone, while the numbers after exercise show exact HR values. The measured numbers are within the normal average resting heart rate between 61 and 76 bpm, and an after exercise fitness range between 98 and 166 bpm **(Figure 4c and d),** highlighting the accuracy of paper-based pressure sensor compared to more sophisticated alternatives. Stress can be measured through the change in the interval between heartbeats, known as heart rate variability (HRV) characterized by pressure peak-to-peak time [32]. Heart rate variability is one of the most robust, non-invasive measures of stress response and is designated by a reduction in HRV (i.e. monotone beats frequency). In fact, in healthy young adults, the interval between heartbeats naturally varies, to the extent that the heart rhythm during a single breath cycle can change by 10 to 15 beats per minute. But when someone is in under stress (agitated, scared, distressed, excited), the autonomic nervous system is triggered, which reduces the variability in the interval between heartbeats. For example, a stressed-out heart may only vary by two beats per breath cycle. Therefore, logging HRV over a 24-hour period can help detect vulnerability to certain mental conditions such as panic attacks. Respiration rate can be also retrieved from the same sensor by measuring the difference in timing between expansions of the chest and abdomen, which can be used to detect a partial airway obstruction. Then, band-pass filters can be used to remove interference from body motion during speaking and walking[33].

In a second experiment, the health monitor was positioned around the left-hand wrist in such a way the pressure sensor is in contact with the radial artery **(Figure 4b).** This careful and intimate placement will allow us to simultaneously measure heart rate, blood pressure, body temperature, and sweat levels in real-time. Under normal resting conditions, we were able to resolve the radial artery pulse waveform over a period of 30 seconds **(Figure 4e)**, from which we determine HR= 72 bpm **(Figure 4f).** Again our measured value was compared to the Samsung S5 heart rate sensor which displayed HR= 73 bpm. The 1% deviation shows consistency between the two methods. Moreover, the arterial waveform clearly resolves the tonometry pulse pressures characterized by distinguishable peaks P1, P2, and P3, respectively corresponding to early systolic blood pressure (SBP), late systolic

augmentation shoulder (late SBP), and early diastolic blood pressure (early DBP) which is preceded by a Dicrotic notch (closure of aortic valve) **(Figure 4g).** The observed three waves within the pulse envelope respectively correspond to an incident wave generated by blood flow (P1) and two reflected waves, one from the hand region (P2) and a later-arriving wave from the lower body (P3)[34]. These variations are caused by constitution of the blood pressure from the left ventricle contracts and reflective waves from the lower body. From the pulse waveform in **Figure 4g**, blood pressure is characterized by the pressure maxima (SBP) and pressure minima (DBP), from which one can calculate the pulse pressure at the surface of the skin and then have an approximate prediction of the absolute blood pressure assuming a the approximate dampening factor in the range between 50% - 70%[29]. In **Figure 4g** DBP is determined to be ≈ 12.12 pF and SBP at ≈ 12.14 pF. For the purpose of this application, we expect the sensor to detect pressures in the kPa range on its surface, thus calibration of the data to absolute pressure values will be based on a pressure sensitivity of 0.0186 $pF.kPa^{-1}$ and an intercept of 12.06 pF. Using this relationship, we calculate a systolic high blood pressure of SBP = 4.32 kPa ≈ 33 mmHg and a diastolic low blood pressure of DBP = 3.25 kPa ≈ 24 mmHg. Applying the dampening range of 70% - 50%, we approximate an original absolute blood pressure values in the range of SBP/ DBP = (65 – 108 mmHg)/ (49 – 81 mmHg). Considering the 70% dampening factor, our approximate measurement of absolute blood pressure is SBP/ DBP = 108 mmHg/81 mmHg, which is categorized under the ideal blood pressure for a male in the age range 15 -18 years old[35], hence confirming the well-being of our volunteer. Understanding the implications of blood pressure measurements is important. Certain medical conditions can be linked to different levels of blood pressure (BP) in the following way[35]: (1) Hypotension when BP is too low (i.e. < 90/60 mmHg), (2) Prehypertension for BP 120/80 to 139/89 mmHg, (3) Hypertension stage 1 when BP ranges from 140/90 to 159/99 mmHg, (4) Hypertension stage 2 when BP is much higher than 160/100 mmHg (e.g. as a result of sleep apnea), and (5) Hypertension crisis when BP is about 180/110 mmHg, in which case the person needs to seek professional help. High blood pressure has major side effects and can be a sign of serious consequences such as heart attack, heart failure, stroke, and kidney

disease[35]. Since the calibration of the sensor will depend from one person to another, and the dampening factor will be changed, this application will be useful for prevention, where the sensor would inform the user whether they have normal BP, or concerning low and high levels that would require proper attention.

Another key advantage of acquiring the complete arterial pulse waveform **(Figure 4g)** is that several hemodynamic parameters can be directly calculated or estimated in real time such as arterial indexes, stroke volume variation, and cardiac output, enabling a profound portrayal of a patient's cardiovascular health and well-being[36]. Arterial stiffness is one of the major health concerns leading to arterial clogging, diabetes, and hypertension. Thus, it is established as a highly reliable predictive parameter for cardiovascular diseases. Arterial stiffness can be identified from the peaks positions in the radial artery waveform. As the elastic arteries become stiffer, pulse wave velocity (PWV) increases and the reflected wave from the lower body returns earlier to the radial artery, migrates up the pressure wave towards peak systolic pressure, and thus causes a decrease in T_{DVP} (digital volume pulse time) and an increase in arterial stiffness index, AI_r[37]. Arterial stiffness can thus be analyzed from the arterial augmentation stiffness index (AI_r), diastolic augmentation index (DAI_r), digital volume pulse (DVP), and PWV **(Equation 5):**

$$AI_r = P2/P1 \quad (5.1)$$

$$DAI_r = P3/P1 \quad (5.2)$$

$$\Delta T_{DVP} = t_{p2} - t_{p1}\ [s] \quad (5.3)$$

$$PWV = \text{body length}/(t_{SBP} - t_{DBP})\ \ [m/s] \quad (5.4)$$

From the measured radial artery waveform, we calculate an average AI_r = 0.52 (52%), DAI_r = 0.37 (37%), ΔT_{DVP} = 270 ms with DVP = 5.83 m/s, and PWV = 6.07 m/s **(Figure 4g).** These numbers are highly related to the age of people, and show to be consistent for a healthy young male[37]. Note that for PWV and DVP calculations, the path length is approximated to the person's height. The time difference t_{13} between the arrival of the primary systolic pulse (P1) and the reflection pulse (P3) is also a measure of arterial stiffness that tracks changes in arterial pulse pressure and beat-by-beat

frequencies, and is measured to be t_{13} = 520 ms **(Figure 4g).** Sleep apnea can be also analyzed and retrieved from arterial stiffness[38]. Large elastic arteries and smaller muscular conduit arteries become stiffer with ageing, a process that is accelerated in the presence of cardiovascular disease (CVD), and obstructive sleep apnoea (OSA) has been increasingly linked with excess cardiovascular morbidity and mortality[38].

Simultaneously, body temperature and sweating (or skin humidity) were measured and analyzed before and after exercise, as seen in **Figure 4h** and **Figure S3**. Real-time measurements for detecting temperature and humidity from the surface of the skin as the volunteer starts exercising are respectively shown in **Figure S3a and b**. After calibration and addition of 5ºC to account for the differences between skin and body temperature values, we calculate a resting body temperature of 36.45 ºC with a slight rise of nearly 0.5 ºC directly after exercise, attributed to the loss of heat from the 70% of energy powering our muscles[39]. The relative humidity of the skin before exercise is measured to be 35% at an ambient relative humidity of 46% RH and temperature of 23 ºC **(Figure 4h).** This result is in agreement with the expected values described in the literature for normal skin hydration levels[40]. After exercise, our heart pumps the heat in the blood from the muscles to the skin, leading to sweat. This highlights the observed increase in relative skin humidity up to 85% **(Figure 4h).**

Our results demonstrate that the subtle differences in radial pulse pressures, body temperature and skin humidity, could be precisely resolved with the presented “Paper Watch”, indicating its potential to serve as a low-cost wearable device for mobile health monitoring and remote diagnostic applications. It is also worth noting that future work would include a study of the behavior of vital signs detection under various environmental conditions with variations in humidity levels and ambient temperatures. This will entail a deep study of the material system of paper (which is non-uniform and anisotropic). We would expect slight effect on the absolute value of the data collected from the sensors (*viz.* a shift up or down in the signal - which can be easily calibrated for), however we do not expect any significant degradation in the sensitivity or performance of our sensors. In fact,

we have shown in our previous report [27] that the cellulose paper used desorbs humidity and dissipates heat very fast (*viz.* fast recovery times enabled the porosity of the platform), enabling our sensors to recover their initial condition within seconds, even with no encapsulation and after cycles of testing in real-time.

6. Paper Watch

In pursuit of an advanced product development integrating the flexible Si IC on paper implementation, we assembled an ultra-low cost Paper Watch. This gadget serves as a fully integrated wearable health monitor for simultaneously detecting the various vital signs in real-time. The system is completely flexible and lightweight, using recyclable paper-based sensors and lightweight processing unit and interface circuitry printed on a flexible PCB board. **Figure 5a** illustrates the layouts of the printed circuitry, for both the microcontroller unit (printed on the top side of the board) and the interface circuitry (printed on the bottom side of the same board). An initial design is to print the described circuitry on a large flexible PCB piece that can be fully wrapped around the wrist, as seen in **Figure 5b.** As a second design, we print the system on a small flexible PCB piece, as illustrated in the digital photos of **Figure 5c** for the controller side and **Figure 5d** for the sensors interface. For the system design and operation, we collect data from the paper sensors through the electronic circuit layout explained in the block diagram in **Figure 5e**. Details about the Watch circuitry can be found in **Supplementary Information**. Finally, to complete the Paper Watch, the PCB assembly was housed in a flexible 3-D printed casing **(Figure 5f),** allowing the device to be customizable and adjustable to varying wrist sizes using an affordable and scalable approach. The paper-based sensors were then placed on the exterior of the Watch as seen in **Figure 5(g-i),** in such a way that they can be in intimate contact with the skin. Note that the pressure sensor was placed further apart around the band in order to interact with the radial artery when the Watch is worn. This compact, lightweight and affordable Watch device will allow continuous and simultaneous monitoring of health vital signs in an unprecedented manner. The use of paper-based sensors permits easy

replacement of the sensors when they are damaged as well as customization of the wearable device where the user can effortlessly replace the sensors through a simple "detachment and taping" technique, maintaining device reliability over the long run.

The presented "Paper Watch" demonstration is a proof of concept design of an ultimate low-cost standalone health monitor device. From a flexible low-cost hardware perspective, our demonstration of the "Paper Watch" is unprecedented. In future work, software optimizations and calibrations of our Paper Watch will be made and a focus on the system level approach will be studied with collection of vital signs from the watch itself.

7. Conclusion

Health monitors should possess three keys features: functionality (multi-sensory, sensitivity, selectivity, recovery, rapidity), convenience (reusability: easy and simple to use, monitor, replace, energy efficiency) and affordability. In this report, we presented a new integration strategy where paper-based sensors have been used for body vitals monitoring, with simultaneous detection of various body vitals in real-time such as heart rate, blood pressure, respiration rate, body temperature and sweating, adopting an approach best suited for intimate adhesion and conformity on the surface of the skin. This intimate attachment is necessary to properly collect information from the body rather than the surroundings. We demonstrate the effectiveness of this integrated sensory system in detecting heart rate, blood pressure, sweating, and body temperature, and revealed its viability in wearables by showing the negligible effect of bending when the system is worn under different bending radii. Furthermore, we have shown a low-cost Paper Watch system level approach highlighting the adoptability of paper sensors into a practical wearable product. We show this through a completely comprehensive approach of a fully flexible standalone system integrating the paper sensors using the most low-cost and customizable packaging approach. The device is lightweight, recyclable, and flexible, perfect for everyday use due to its conformity to the body. This is presumably the first demonstration of a fully autonomous (non-functionalized recyclable paper based multi-sensors with

flexible silicon ICs), low-cost and recyclable health monitoring system showing potential for manufacturability, scalability, and customization. Numerous health concerns and diseases can be identified through this type of real-time basic monitoring, where early detection of potentially serious illnesses may be realized through a combination of concerns revealed from the health monitor. We have shown, future of paper electronics will allow changes in health conditions to be predicted prior to noticing symptoms. This "prediction" and "therapy" by wearable health-monitoring systems should be the next class of electronics and open a new door for health-monitoring applications.

8. Experimental Section

Measurement Setup: Real-time data from the Paper Health Monitor was collected using a Keithley 4200™ semiconductor analyzer. Body temperature was measured by applying a constant current bias of 10 mA and sampling voltage every 130 ms. Sweating was monitored by applying 1 MHz modulation frequency and 100 mV AC voltage. Capacitance values were then collected with respect to time at a sampling rate of 130 ms. Similarly, we detect heart rate and blood pressure by monitoring capacitance changes with a sampling rate of 30 ms. To reduce noise interference in the after exercise measurements, we ran a Fast Fourier Transform (FFT) to identify the required range of frequencies. Based on our results, we post-processed the original plot using band bass filtering for frequencies in the interval of [1-7 Hz].

Supporting Information

Supporting Information is available from the Wiley Online Library or from the author.

Acknowledgements

We thank Swnalund Chair Professor of University of Illinois at Urbana-Champaign Prof. John Rogers for useful discussion about this paper. This publication is based upon work supported by the King Abdullah University of Science and Technology (KAUST) Office of Sponsored Research (OSR) under Award No. Sensor Innovaiton Initiative OSR-2015-Sensors-2707 and KAUST-KFUPM Special Initiative OSR-2016-KKI-2880. MMH conceptualized and directed the study. JMN lead the study. KM developed the electronic circuit. KL assisted with human subject testing. AAA helped with design. JMN and MMH co-authored the paper. Every author reviewed the final draft.

Received: ((will be filled in by the editorial staff))
Revised: ((will be filled in by the editorial staff))
Published online: ((will be filled in by the editorial staff))

[1] Y. Khan, A. E. Ostfeld, C. M. Lochner, A. Pierre, A. C. Arias, *Adv. Mater.* **2016**, *28*, 22.

[2] K. Takei, W. Honda, S. Harada, T. Arie, S. Akita, *Adv. Healthcare Mater.* **2015**, *4*, 4.

[3] G. Appelboom, E. Camacho, M. E. Abraham, S. S. Bruce, E. L. Dumont, B. E. Zacharia, R. D'Amico, J. Slomian, J. Y. Reginster, O. Bruyère, *Arch. Public Health* **2014**, *72*, 1.

[4] O. D. Lara, M. A. Labrador, *IEEE Commun. Surv. Tutor.* **2013**, *15*, 3.

[5] G. Schwartz, B. C.-K. Tee, J. Mei, A. L. Appleton, D. H. Kim, H. Wang, Z. Bao, *Nat. Commun.* **2013**, *4*.

[6] M. Raj, S. Patel, C. H. Lee, Y. Ma, A. Banks, R. McGinnis, B. McGrane, B. Morey, J. B. Model, P. DePetrillo, in *Stretchable Bioelectronics for Medical Devices and Systems*, Springer, **2016**, pp. 193-205.

[7] T. Q. Trung, N. E. Lee, *Adv. Mater.* **2016**, *28*, 22.

[8] X. Huang, Y. Liu, H. Cheng, W. J. Shin, J. A. Fan, Z. Liu, C. J. Lu, G. W. Kong, K. Chen, D. Patnaik, *Adv. Funct. Mater.* **2014**, *24*, 25.

[9] M. K. Choi, O. K. Park, C. Choi, S. Qiao, R. Ghaffari, J. Kim, D. J. Lee, M. Kim, W. Hyun, S. J. Kim, *Adv. Healthcare Mater.* **2016**, *5*, 1.

[10] T. Someya, Y. Kato, T. Sekitani, S. Iba, Y. Noguchi, Y. Murase, H. Kawaguchi, T. Sakurai, *Proc. Natl. Acad. Sci. U.S.A.* **2005**, *102*, 35.

[11] C. M. Boutry, A. Nguyen, Q. O. Lawal, A. Chortos, S. Rondeau‐Gagné, Z. Bao, *Adv. Mater.* **2015**, *27*, 43.

[12] J. W. Jeong, W. H. Yeo, A. Akhtar, J. J. Norton, Y. J. Kwack, S. Li, S. Y. Jung, Y. Su, W. Lee, J. Xia, *Adv. Mater.* **2013**, *25*, 47.

[13] D.-H. Kim, N. Lu, R. Ma, Y.-S. Kim, R.-H. Kim, S. Wang, J. Wu, S. M. Won, H. Tao, A. Islam, *Science* **2011**, *333*, 6044.

[14] C. L. Choong, M. B. Shim, B. S. Lee, S. Jeon, D. S. Ko, T. H. Kang, J. Bae, S. H. Lee, K. E. Byun, J. Im, *Adv. Mater.* **2014**, *26*, 21.

[15] Y. Shu, C. Li, Z. Wang, W. Mi, Y. Li, T.-L. Ren, *Sensors* **2015**, *15*, 2.

[16] S. C. Mukhopadhyay, *IEEE Sens. J.* **2015**, *15*, 3.

[17] M. M. Rodgers, V. M. Pai, R. S. Conroy, *IEEE Sens. J.* **2015**, *15*, 6.

[18] Y. Zang, F. Zhang, C.-a. Di, D. Zhu, *Mater. Horiz.* **2015**, *2*, 2.

[19] R. C. Webb, A. P. Bonifas, A. Behnaz, Y. Zhang, K. J. Yu, H. Cheng, M. Shi, Z. Bian, Z. Liu, Y.-S. Kim, *Nat. Mater.* **2013**, *12*, 10.

[20] Y. Wang, L. Wang, T. Yang, X. Li, X. Zang, M. Zhu, K. Wang, D. Wu, H. Zhu, *Adv. Funct. Mater.* **2014**, *24*, 29.

[21] S. Gong, W. Schwalb, Y. Wang, Y. Chen, Y. Tang, J. Si, B. Shirinzadeh, W. Cheng, *Nat. Commun.* **2014**, *5*, 3132.

[22] A. Chortos, Z. Bao, *Mater. Today* **2014**, *17*, 7.

[23] W. Gao, S. Emaminejad, H. Y. Y. Nyein, S. Challa, K. Chen, A. Peck, H. M. Fahad, H. Ota, H. Shiraki, D. Kiriya, *Nature* **2016**, *529*, 7587.

[24] A. M. Hussain, M. M. Hussain, *Adv. Mater.* **2016**, *28*, 22.

[25] M. M. Hamedi, A. Ainla, F. Güder, D. C. Christodouleas, M. T. Fernández‐Abedul, G. M. Whitesides, *Adv. Mater.* **2016**, *28*, 25.

[26] G. A. T. Sevilla, J. P. Rojas, H. M. Fahad, A. M. Hussain, R. Ghanem, C. E. Smith, M. M. Hussain, *Adv. Mater.* **2014**, *26*, 18.

[27] J. M. Nassar, M. D. Cordero, A. T. Kutbee, M. A. Karimi, G. A. T. Sevilla, A. M. Hussain, A. Shamim, M. M. Hussain, *Adv. Mater. Technol.* **2016**, *1*, 1.

[28] B. Nie, S. Xing, J. D. Brandt, T. Pan, *Lab Chip* **2012**, *12*, 6.

[29] R. E. Klabunde, "Cardiovascular Physiology Concepts", can be found under http://www.cvphysiology.com/Blood%20Pressure/BP019.htm, 2016.

[30] K. Niskanen, Mechanics Of Paper Products, Walter De Gruyter, Berlin, 2012.

[31] A. P. Avolio, M. Butlin, A. Walsh, *Physiol. Meas.* **2009**, *31*, 1.

[32] M. Malik, *Ann. Noninvasive Electrocardiol.* **1996**, *1*, 2.

[33] G. K. Prisk, J. Hammer, C. J. Newth, *Pediatr. Pulmonol.* **2002**, *34*, 6.

[34] T. H. Marwick, T. C. Gillebert, G. Aurigemma, J. Chirinos, G. Derumeaux, M. Galderisi, J. Gottdiener, B. Haluska, E. Ofili, P. Segers, *Eur. Heart J. Cardiovasc. Imaging* **2015**, *16*, 6.

[35] V. Marchione, "Blood pressure chart: Understanding blood pressure readings by age and gender", can be found under http://www.belmarrahealth.com/understanding-blood-pressure-readings-is-key-to-overall-well-being/, 2015.

[36] E. S. Muxfeldt, R. Fiszman, C. H. Castelpoggi, G. F. Salles, *Hypertension Res.* **2008**, *31*, 4.

[37] F. Fantin, A. Mattocks, C. J. Bulpitt, W. Banya, C. Rajkumar, *Age Ageing* **2007**, *36*, 1.

[38] C. L. Phillips, M. Butlin, K. K. Wong, A. P. Avolio, *Sleep Med. Rev.* **2013**, *17*, 1.

[39] R. Lenhardt, D. I. Sessler, *Anesthesiology* **2006**, *105*, 6.

[40] R. Mole, *J. Physiol.* **1948**, *107*, 4.

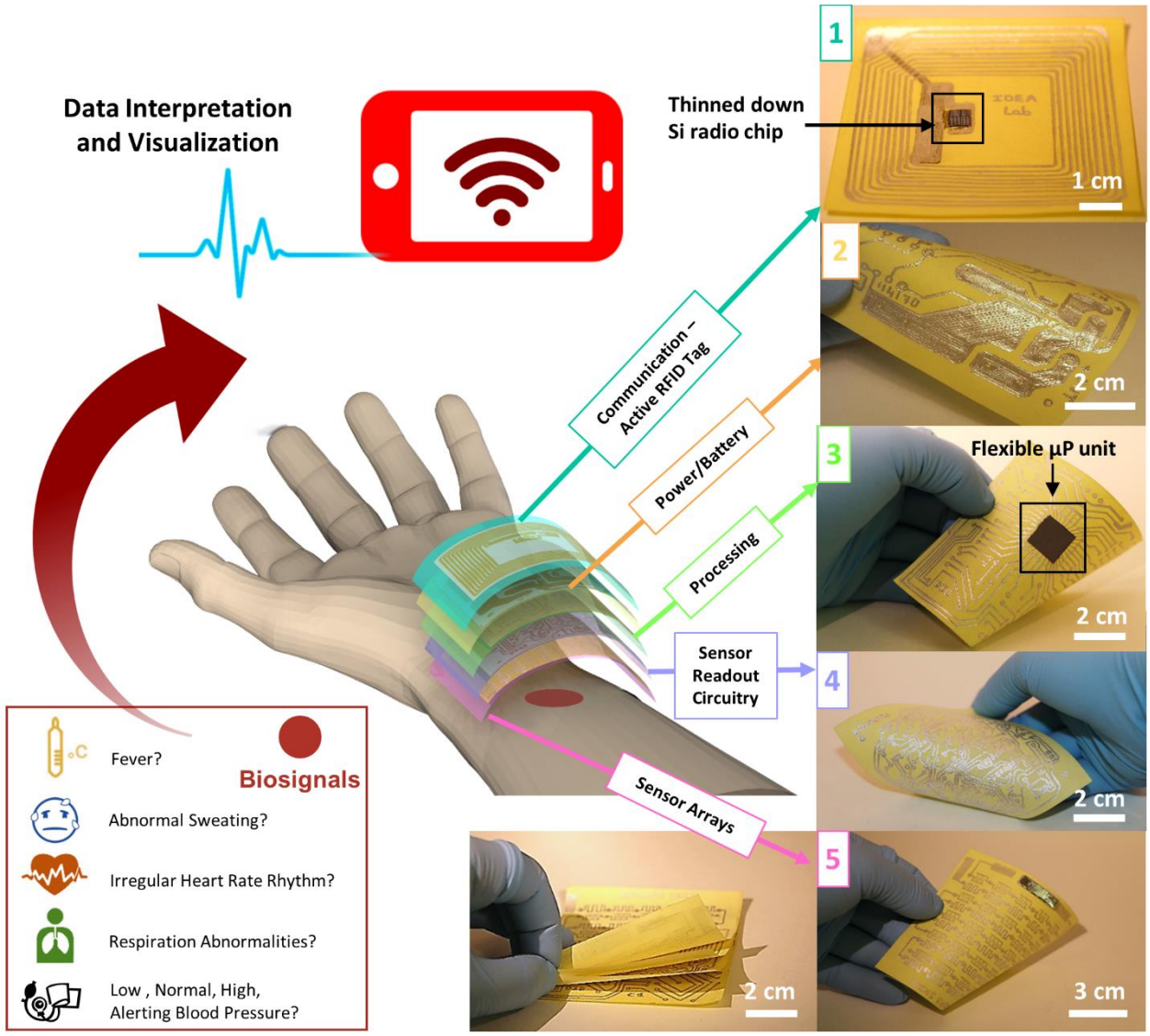

Figure 1. Conceptual demonstration of 3D stacked paper-based autonomous healthcare monitoring system integration, capable of monitoring various critical bio signals from one singular point around the wrist. Each layer is fully printed on cellulose paper using silver ink for interconnects, and thinned down flexible Si-based chips for the active components of the circuitry where high performance processing using state-of-the-art technology is required. Beginning from the top, layer **[1]** represents the digital photo of an active RFID tag printed on paper with a flexible Si-based radio chip for wireless data communication; layer **[2]** shows the digital image of a power source printed circuitry; layer **[3]** displays the processing unit where a flexible Si-based microprocessor (µP) die is integrated through flip-chip with the rest of the printed circuitry on paper; layer **[4]** illustrates the sensors readout circuitry fully printed on paper; and layer **[5]** is composed of the multifunctional healthcare sensory platform we are presenting in this work. As shown in the corresponding digital photo, the sensory layer needs to be in direct contact with the skin, essential for collection of bio signals from the surface of the skin. Finally, data collected from the sensors is wirelessly transmitted to a smartphone application where vital signs can be simultaneously interpreted and visualized in real-time.

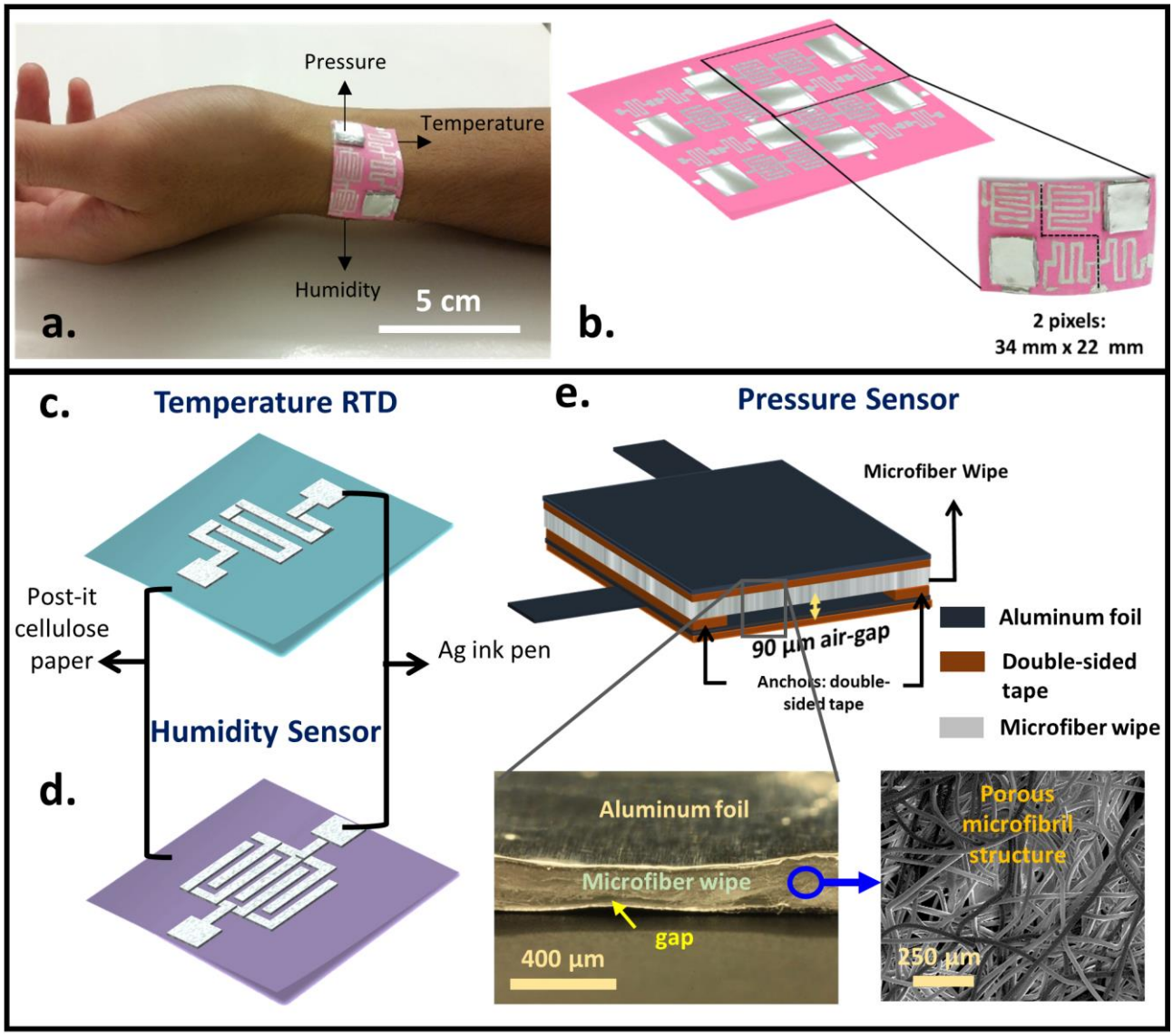

Figure 2. Paper health monitor patch: (a) Digital photo of the multifunctional paper-based health sensors for vital signs monitoring. (b) Schematic of the paper health monitor (34 mm × 22 mm) illustrating the in-plane monolithic integration of temperature, humidity and pressure sensors. (c) Schematic showing the fabrication design of resistive temperature sensor (RTD). (d) Schematic showing the design and materials used for humidity sensor. (e) Schematic of the pressure sensor design where the compressive pressure sensing dielectric is composed of a microfiber wipe and an air-gap. Zoom-in digital photo displaying the cross-section image of the process sensor with an outset scanning electron microscopy (SEM) image highlighting the porous long microfiber structure of the cleanroom wipe used.

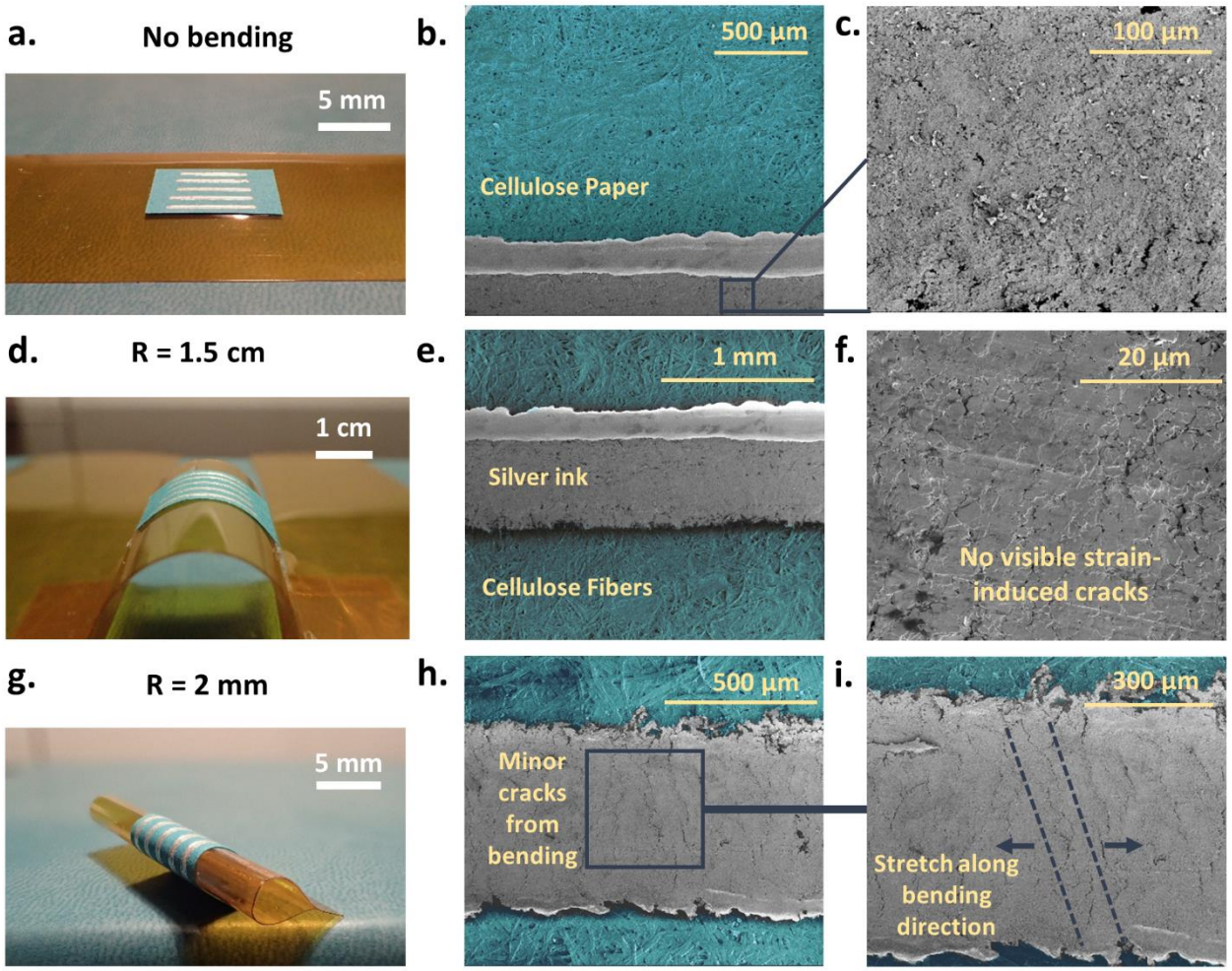

Figure 3. Bending effects on silver metal interconnects on flexible paper. (a) Digital photo of silver ink lines (≅ 5 µm thick) drawn on cellulose post-it paper. (b) and (c) Corresponding scanning electron microscopy (SEM) images showing the uniformity of the silver ink film under no bending at different magnification levels. (d) Digital photo of the same sample bent down to a bending radius R = 1.5 cm. (e) and (f) Corresponding SEM pictures highlighting no strain-induced cracks in the silver metal film due to very minimal induced strain. (g) Digital photograph of the sample bent down to R = 2 mm. (h) and (i) The SEM images for a sample bent at R = 2 mm shows visible cracks induced in the silver film, even at low magnifications.

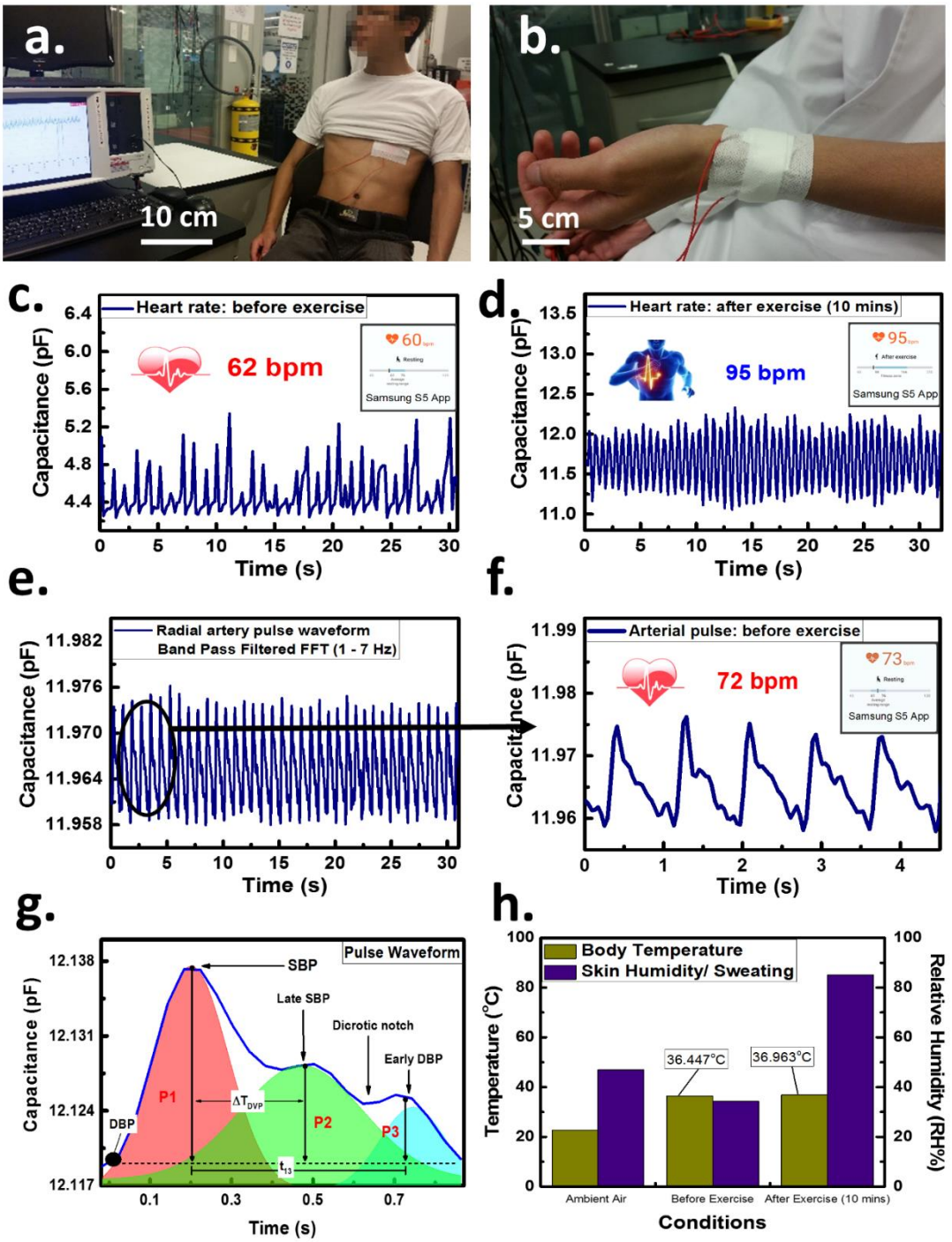

Figure 4. Real-time body vitals monitoring. (a) Digital photo showing the setup for heart rate monitoring by placing the paper health monitor on the chest near the heart. (b) Digital photo showing paper health monitor wrapped around the wrist for intimate vital signs monitoring simultaneously and in real-time. (c) Heart rate pressure profile before exercise, with comparative digital photo inset taken from Samsung S5 "S Health" application. (d) Heat rate detection after exercise, with inset from "S Health" monitoring application. (e) Radial artery pressure pulse waveform detected throughout a period of 30 seconds, and band pass filtered between 1 and 7 Hz for noise elimination. (f) Resting heart rate detection from arterial pulse monitoring around the wrist. (g) Blood pressure and arterial stiffness detection from resolvable peaks of the pressure radial artery waveform. (h) Histogram displaying simultaneous sensing of body temperature and skin humidity or sweat levels before and after exercise.

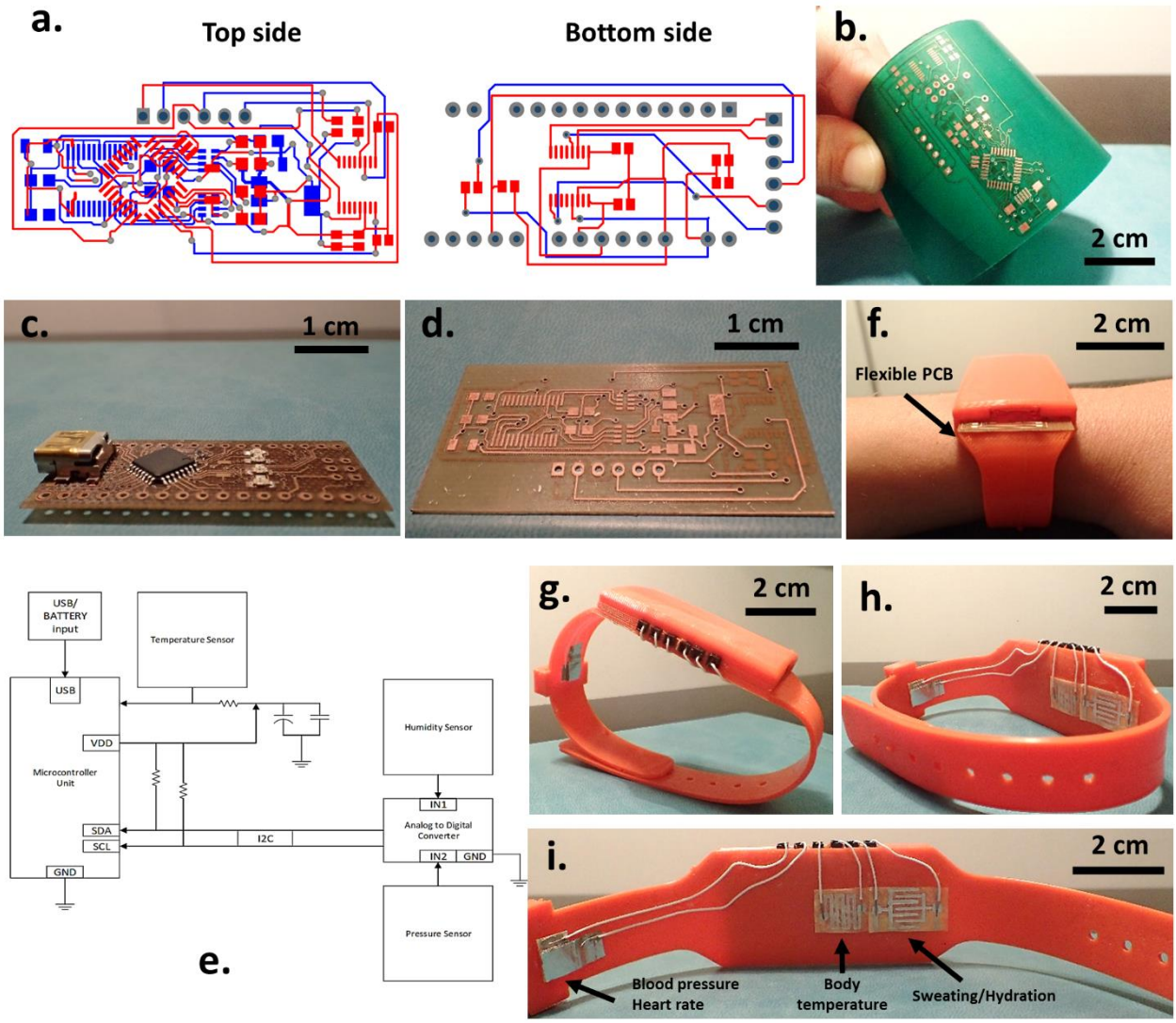

Figure 5. "Paper Watch" prototype for continuous health monitoring. (a) Layout of the printed circuitry on each side of the flexible PCB: the top side represents the microcontroller unit and the bottom side shows the interface circuitry. (b) Digital photo of the first design where the full system is printed on a flexible PCB band. (c) Digital photo of the microprocessing unit printed on a flexible PCB, and (d) illustrates the digital photograph of the sensors readout interface circuitry printed on the opposite side of the same small flexible PCB piece as the processor. (e) Block diagram schematic of the full system integration. (f) Digital photo of the Paper Watch prototype where the flexible PCB piece is inserted in a 3D printed wristband package. (g), (h) and (i) digital photographs of the Health Paper Watch, illustrating the attachment of the paper sensors in such a way they are in close contact with the skin and the pressure sensor is in contact with the radial artery around the wrist.

Supporting Information

Title: Recyclable Non-functionalized Paper Based Ultra-Low Cost Wearable Health Monitoring System

*Joanna M. Nassar[1], Kush Mishra[1], Kirk Lau[1, 2], Andres A. Aguirre-Pablo[3] and Muhammad M. Hussain[1]**

J. M. Nassar, Kush Mishra, Kirk Lau, Prof. M. M. Hussain
[1]Integrated Disruptive Electronic Applications (IDEA) Lab and Integrated Nanotechnology Lab, Computer Electrical Mathematical Science and Engineering Division, King Abdullah University of Science and Technology (KAUST), Thuwal 23955-6900, Saudi Arabia

Kirk Lau
[2]Harvey Mudd College, Claremont, CA 91711, USA

Andres A. Aguirre-Pablo
[3]High Speed Fluids Imaging Lab, Physical Sciences and Engineering, Mechanical Engineering, Physical Science and Engineering Division, King Abdullah University of Science and Technology (KAUST), Thuwal 23955-6900, Saudi Arabia

Corresponding author's e-mail: muhammadmustafa.hussain@kaust.edu.sa

1. Materials and Methods

Paper Health Monitor Fabrication

The sensors patch is a 3.5 × 2.5 cm paper platform consisting of a series in-plane integration of pressure/force, humidity and temperature sensors. Temperature sensors are fabricated by drawing a 1 x 1 cm^2 resistive structure using Circuit Scribe™ silver ink pen on 3M Post-it Note paper. Similarly, using the same pen, humidity sensors consist of a 1 x 1 cm^2 interdigitated electrodes structure with 2 mm finger width and 1 mm finger separation, where the paper acts as well as the humidity sensing film. Finally, 1 x 1 cm^2 pressure sensors were built through a parallel plate capacitor design, and incorporating a 90 µm air-gap. The bottom contact pad consists of a 1 x 1 cm^2 aluminum foil taped on the paper using double-sided adhesive tape. Then, we introduce the air gap by depositing two 1 cm x 2 mm strips of double-sided tape (d_{tape} = 90 µm) on either side of the bottom electrode. We then

continue by placing our pressure sensing dielectric material consisting of a porous 100% polypropylene microfiber cleanroom wipe ($d_{fiber\text{-}wipe}$ = 600 µm) (Berkshire™ PRO-WIPE™ 880). Finally, we finish by taping a 1 x 1 cm^2 aluminum foil top contact using a 1 x 1 cm^2 sheet of double-sided adhesive tape.

Materials Properties

Aluminum foil is used for its intrinsic conductive property ($\rho = 3.83 \times 10^{-8}\ \Omega.m$), whereas microfiber wipe (Berkshire PRO-WIPE 880) is used due to its naturally porous polypropylene (PP) fibers structure (*viz.* PP material density D_{PP}= 0.91 $g.cc^{-1}$) [1] and sensitive deformation with low pressure sensitivity of $S_{1,wipe}$ = 0.61 $pF.kPa^{-1}$ under applied pressures from 9 Pa to 200 Pa [2]. Cellulose paper was also chosen due to its flexibility (elastic modulus ~ 5 GPa and tensile strength ~ 52 MPa [3], where flexural/bending modulus ≈ elastic modulus) and recyclability (Grade 1, recycled with mixed paper materials [4, 5]) but also owing to its highly porous medium (contains as much as 70% air [6]) that displays benefits for rapid humidity sensing [2, 7]. Moreover, for scalability purposes, we have chosen to use a silver ink pen (Circuit Scribe) to draw very fine metal lines of 500 µm width, indicating a sheet resistance of 0.05–0.2 Ω/sq on cellulose paper. This resistive property of the temperature sensor is associated to the length of the structure and inversely varies with the thickness of the conductor. The sensitivity depends on the conductivity of the material used, and is slightly affected by the thickness and porosity of the film [2]. As for the humidity sensor structure, the size of the conductive fingers and the gap distance in between affects the capacitance value of the sensor.

2. Detection Technique of Vital Signs

2.1 Respiration Rate

Respiration rate is a critical vital sign since it is a measure of your inflow of oxygen and removal of carbon dioxide. Abnormal respiration rates can be symptoms of many disorders such as sleep apnea, asthma, chronic obstructive pulmonary disease, and anemia [8, 9]. Typical respiration rate at rest ranges

from 12 to 20 breaths per min, and at anything below 12 breaths per min or above 25 breaths per min is considered abnormal [10]. To measure respiration rate, most wearable respiration sensors are placed on the chest or abdomen, and physically expand and contract along with the lungs. Thus, typical sensors to be employed are strain or pressure sensors that can respond to force induced due to expansion of the lungs during breathing. In our case, we use a capacitive pressure sensor placed on the chest. During expansion of the lungs, the dielectric material is physically deformed with the contraction and expansion of the chest (where thickness is reduced), thus with each breath, we detect a peak in the pressure via an increase in the capacitance of the sensor. Again, this mechanism requires the sensor to be in close contact with the body so that the expansion and contraction of the torso during breathing is properly transmitted to the sensor. Therefore, it is critical for the sensor to be as comfortable, conformal, and lightweight as possible.

2.2 Skin and Body Temperature

Body temperature must be monitored to ensure safe and effective care. It provides an insight into the physiological state of a person. An elevated body temperature can be an indication of infection or fever, whereas a cold body temperature can indicate a low blood flow due to circulatory shock [11]. When the body is too hot, the blood vessels in the skin expand to carry the excess heat to the surface of the skin, allowing us to effectively monitor elevated body temperature from the surface of the skin [12]. Nevertheless, body temperature (T_{BT}) is different from skin temperature (T_{skin}) ($T_{skin} < T_{BT}$), and in common practice, people measure skin temperature even when using a traditional thermometer, and often corrections need to be accounted for to read the proper value. Therefore, when measuring body temperature, the effect of the measurement site needs to be taken into account since skin tissues maintain different temperatures (i.e. body cells manufacture heat in different amounts), leading to internal gradient in heat distribution across the body [12]. On average, the clinically accepted body-core temperature varies from 36 ^{o}C to 37.5 ^{o}C [13].

2.3 Sweating

When body temperature is elevated and the skin's surface carries excess heat, the body begins to sweat by evaporating water as a form of releasing extra energy and restoring back to equilibrium state. And as the sweat evaporates, this helps the body to cool down. In contrast, when the body is too cold, the blood vessels contract so that blood flow to the skin is reduced to conserve body heat [14]. When we place our paper humidity sensor on the surface of a dry skin, the corresponding relative permittivity would be that of our normal skin. As we start sweating, water droplets will accumulate on the surface of the skin and adsorb on the surface of our sensing material (i.e. the paper). In this case, we would read an increase in the relative permittivity of the paper due to the increased water content on the surface of the skin.

2.4 Heart Rate

Heart rate (HR) or pulse is expressed as beats per minute (b.p.m) and is the frequency of cardiac cycles, where the cardiac cycle consists of cycling deoxygenated blood through the lungs and pumping newly oxygenated blood to the body through the aorta [11]. Electrocardiography (ECG) is the conventional method practiced in clinical use, however this technique is not practical for constant use in wearables and can cause skin irritation from the gel electrodes [11]. Electrical, optical or pressure sensing techniques can be used to detect HR via strain or pressure sensors [11, 15]. Heart beat dynamics can also reveal significant amount of information including real-time personalized emotional responses and stress detection.

2.5 Blood Pressure

Blood pressure is one of the most important signs of the general health of a person. A typical blood pressure measurement device is a sphygmomanometer typically wrapped around the arm. However, this technique is not particularly wearable for continuous long-term monitoring, and cardiac conditions may go undetected until a heart attack or stroke occurs. Moreover, the

sphygmomanometer technique lacks the resolution of monitoring the pressure of the pulse waveform in between systolic and diastolic pressure, which is referred to as arterial tonometry, very useful in detecting arterial stiffness index and diagnosing cardiac conditions [16].

Furthermore, it is important to note that in wearable sensors, we are not detecting the actual blood pressure occurring in our arteries, instead, they are detecting the residual pressure effect at the surface of the skin after traveling through several dampening mediums, mainly the thick epidermis of the skin. This dampening effect is a variable that depends on each individual's skin type and thickness, and hence cannot be accurately determined. Nevertheless, the dampening effect can be addressed by comparing the measured pressure values to the blood pressure retrieved from the cuffing technique.

The demonstrated Paper Health Monitor delivers all necessary sensory functionalities needed to develop a preventive healthcare monitoring system. It continuously monitors body vitals such as heart rate, blood pressure, arterial stiffness, body temperature and sweating, simultaneously and in real-time.

3. Real-time Monitoring of Body Vitals

The pressure sensor demonstrated a sensitivity of 0.043 kPa^{-1} in the low pressure regimes of this application [2] (hundreds of Pascal range) and a sensitivity of 0.0186 $pF.kPa^{-1}$ for higher pressure regimes from couple of Kilopascals (kPa) up to 30 kPa **(Figure S4)**. Temperature sensors showed a sensitivity of 0.0107 $\Omega.^{o}C^{-1}$ or a TCR of 0.00372 $^{o}C^{-1}$, and the humidity sensor displayed on average a sensitivity of 0.86 fF/%RH or 0.18 %/ %RH for relative humidity levels up to 97 %RH [2].

4. Paper Fitbit

The Fitbit circuitry has the following inputs: (1) USB or battery input of -5V, (2) temperature sensor data as a resistive input, (3) humidity sensor data as a capacitive input, (3) pressure sensor data as a capacitive input, and (4) outputs through USB serial communication to laptop. The circuit consists of a microcontroller board unit to collect information through digital input pins. The

controller is connected to the temperature sensor through a voltage divider circuit. The analog data acquired from the voltage divider through the microcontroller pin is converted to temperature data. The controller takes digital input from the analog to digital converter (ADC) which in our case is specifically designed for capacitive inputs. The capacitive sensors that measure pressure and humidity are connected as inputs to the ADC and the digital output communicates to the controller through I2C lines. The whole setup was protected from magnetizing in rush currents through parallel capacitances on the input power. LED on the PCB is also used to indicate the power activity and data communication status of the circuit. The output from the printed control board logs data simultaneously and in real-time from all the sensors and displays it through a MATLAB program.

SI References

[1] N. Balasubramanian, "Textile Industry Articles: Polyester vs. Polypropylene", can be found under http://www.fibre2fashion.com/industry-article/textile-industry-articles/polyester-vs-polypropylene/polyester-vs-polypropylene1.asp, 2015.

[2] J. M. Nassar, M. D. Cordero, A. T. Kutbee, M. A. Karimi, G. A. T. Sevilla, A. M. Hussain, A. Shamim, M. M. Hussain, *Adv. Mater. Technol.* **2016**, *1*, 1.

[3] K. Niskanen, Mechanics Of Paper Products, Walter De Gruyter, Berlin, 2012.

[4] "Paper Stock Grades for Green Recycling", can be found under https://www.completerecycling.com/resources/paper-recycling/stock-grades.

[5] "Because You Asked: Can I Recycle Sticky Notes?", can be found under https://livegreen.recyclebank.com/because-you-asked-can-i-recycle-sticky-notes, 2015.

[6] H. Goyal, "Properties of Paper, (Paper Properties)", can be found under http://www.paperonweb.com/paperpro.htm.

[7] D. Shou, L. Ye, J. Fan, K. Fu, *Langmuir* **2013**, *30*, 1.

[8] S. D. Min, Y. Yun, H. Shin, *IEEE Sens. J.* **2014**, *14*, 9.

[9] O. Atalay, W. R. Kennon, E. Demirok, *IEEE Sens. J.* **2015**, *15*, 1.

[10] A. Schringer, L. Goldman, in *Cecil Textbook Of Medicine* (L. Goldman 23rd Ed.), Saunders Elsevier, Philadelphia, 2007.

[11] Y. Khan, A. E. Ostfeld, C. M. Lochner, A. Pierre, A. C. Arias, *Adv. Mater.* **2016**, *28*, 22.

[12] R. Lenhardt, D. I. Sessler, *Anesthesiology* **2006**, *105*, 6.

[13] L. McCallum, D. Higgins, *Nurs. Times* **2011**, *108*, 45.

[14] M. van Dooren, J. H. Janssen, *Physiol. Behav.* **2012**, *106*, 2.

[15] K. Takei, W. Honda, S. Harada, T. Arie, S. Akita, *Adv. Healthcare Mater.* **2015**, *4*, 4.

[16] A. P. Avolio, M. Butlin, A. Walsh, *Physiol. Meas.* **2009**, *31*, 1.

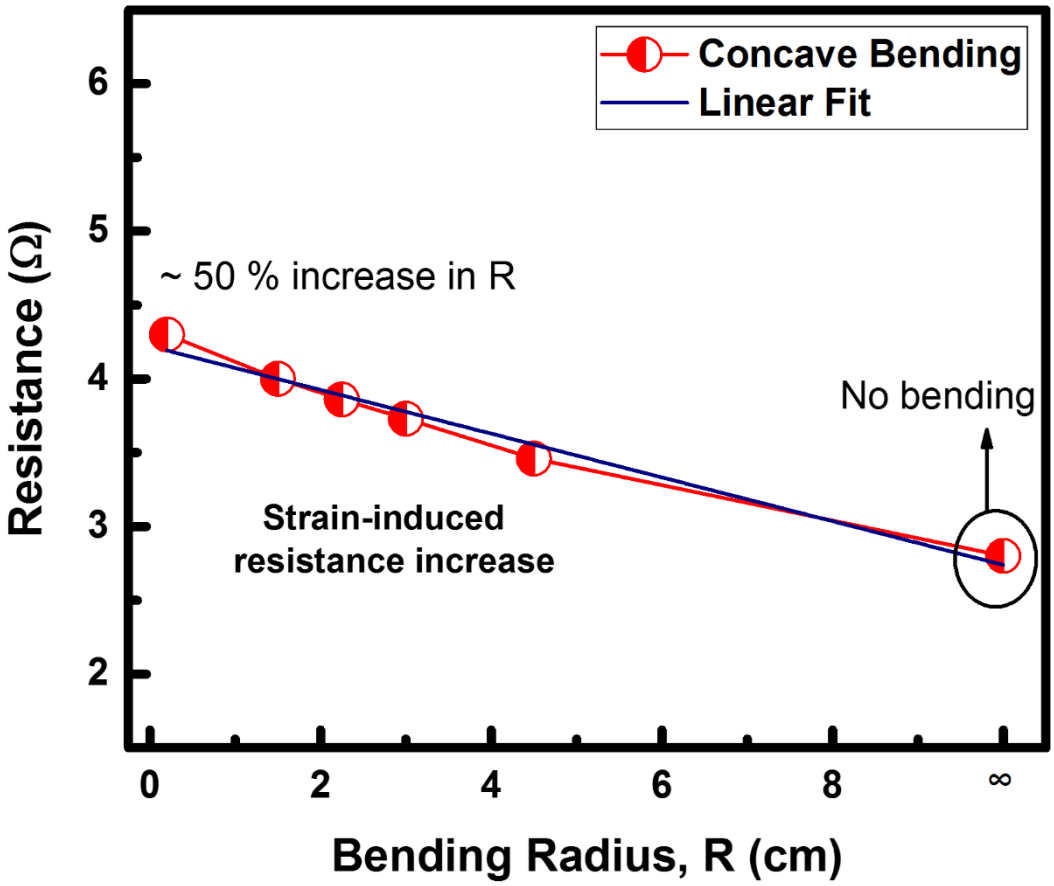

Figure S1. Bending effect on the electrical properties of silver ink. Electrical resistance as a function of varying tensile bending radius of the silver ink lines.

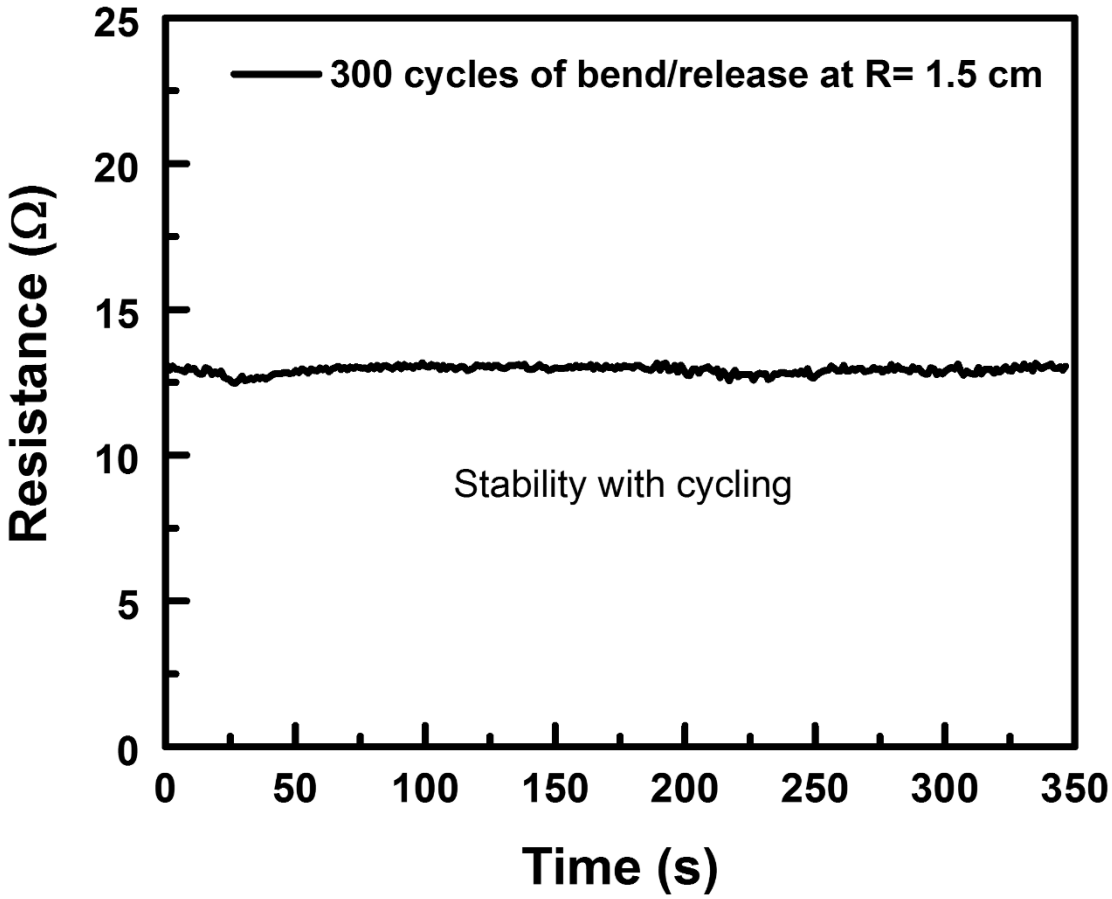

Figure S2. Cycling plot highlighting the stability of the temperature sensor as it is bent down to R= 1.5 cm and unbent for 300 cycles.

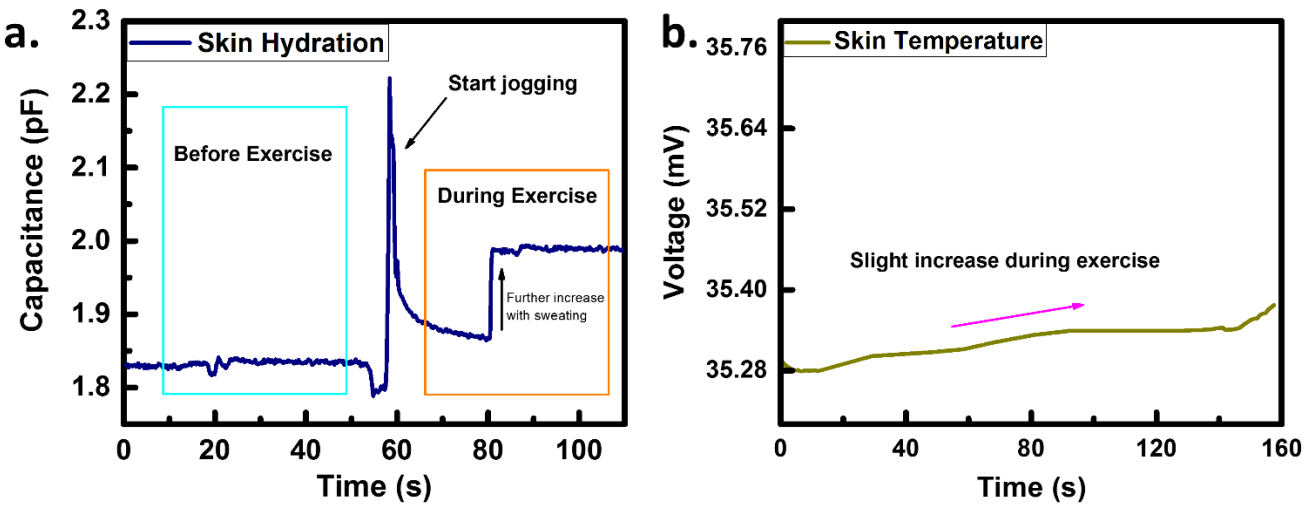

Figure S3. (a) Real-time plot showing the detection and increase in skin hydration due to sweating as the volunteer starts jogging. (b) Real-time plot correspondingly shows the slight increase in the skin temperature of the volunteer as he starts exercising.

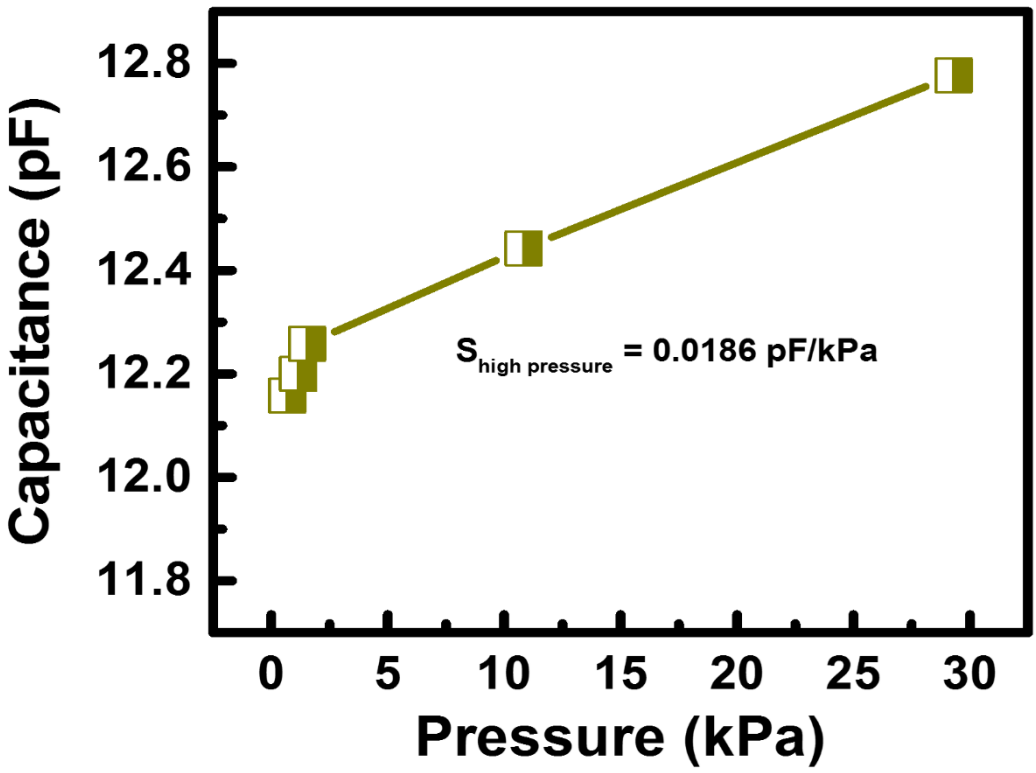

Figure S4. Pressure sensor characteristics. Sensitivity plot over a large range of applied pressures in the kilopascal regime.

Click here to access/download

Production Data

Production data paper.docx